Recombination dynamics in dry-etched (Cd,Zn)Se/ZnSe nanostructures: Influence of exciton localization

K. Herz, G. Bacher, and A. Forchel
Technische Physik, Universität Würzburg, D-97074 Würzburg, Germany

H. Straub, G. Brunthaler, W. Faschinger, and G. Bauer
Institut für Halbleiterphysik, Universität Linz, A-4040 Linz, Austria

C. Vieu
Laboratoire des Microstructures et de Microelectronique, CNRS, 196 Avenue H. Ravera, F-92225 Bagneux, France
(Received 24 April 1998)

The influence of exciton localization on the recombination dynamics in dry etched (Cd,Zn)Se/ZnSe wires and dots has been studied using time-resolved photoluminescence spectroscopy. The observed size and temperature dependence of the excitonic lifetime can be explained quantitatively taking into account the interplay between nonradiative carrier loss at the sidewalls and trapping of free excitons into localized states. From the data, a density of localized states $N_L = 7 \times 10^8$ cm^{-2} and an average localization energy $E_A = 2.8$ meV can be deduced. [S0163-1829(99)13703-2]

I. INTRODUCTION

In low-dimensional semiconductor structures, fluctuations of the composition and/or the size[1,2] result in a spatial variation of the band gap. Especially at low temperatures, excitons can be trapped in such localization centers, suppressing the lateral exciton diffusion. To give an example, it was found that fluctuations of the well width strongly affect, e.g., the photoluminescence (PL) spectrum,[3] the radiative lifetime of excitons,[4,5] the exciton scattering,[6] or the biexciton formation process[7] in quantum wells. Reducing the dimensionality further to quantum wires and quantum dots, the influence of localized states caused by interfaces and/or surfaces on the optical properties is even expected to increase due to an enhanced interface/surface to volume ratio.[8]

A straightforward approach to realize quasi-one-dimensional or quasi-zero-dimensional structures is electron beam lithography followed by an etching process. Even for II-VI materials, this process is well established now, allowing a flexible control of size and geometry in wire and dot structures.[9–12] For this kind of nanostructure, another aspect of surfaces plays an important role: Excitons can recombine nonradiatively via surface states. In deep etched wires and dots, the reduction of the exciton lifetime and the normalized PL intensity with decreasing size is usually explained by a diffusion of free excitons to the sidewalls followed by a nonradiative recombination process at the surface.[9–11,13–18] This picture is confirmed by experimental data, e.g., for GaAs/(Al,Ga)As wires[14,16] and dots,[18] ZnSe/Zn(Se,S) wires,[17] and CdTe/(Cd,Zn)Te wires.[10] However, there are recent reports on (Cd,Zn)Se/ZnSe wire structures,[17,19] where the recombination lifetime observed in time-resolved PL spectroscopy remains approximately constant even if the lateral size is reduced down to 20 nm. Exciton localization caused by alloy or well width fluctuations was supposed to be responsible for this behavior, but there was no quantitative analysis of the experimental data.

In order to explain the size dependence of the exciton lifetime in more detail it seems therefore necessary to develop a uniform picture for the recombination dynamics in deep etched nanostructures describing the interplay between exciton localization and nonradiative loss of free excitons at the sidewalls. In this paper we present a study of the exciton recombination dynamics in dry etched (Cd,Zn)Se/ZnSe wire and dot structures using time-resolved PL spectroscopy. By varying the size and the geometry of the nanostructures the surface/volume ratio is systematically changed. An extended diffusion model including exciton localization and nonradiative carrier loss is developed to describe the experimental data, giving access, e.g., to the density of localized states and the average exciton localization energy.

II. SAMPLE PREPARATION AND EXPERIMENT

The (Cd,Zn)Se/ZnSe quantum well (QW) structure under investigation was grown by molecular-beam epitaxy on a GaAs substrate. The sample consists of a 1.1 μm thick ZnSe buffer, a 10 nm $Cd_{0.20}Zn_{0.80}Se$/ZnSe QW, and a 100 nm ZnSe cap layer. Arrays of wires and dots with different lateral sizes were defined in a polymethylmethacrylate resist (PMMA) by electron beam lithography and transferred into the semiconductor by a reactive ion etching (RIE) process using a CH_4/H_2 gas mixture. Further details were reported elsewhere.[20] Wires and dots with different lateral extension were realized on the same sample allowing a direct comparison of nanostructures with different dimensions.

The excitons recombination dynamics in deep etched nanostructures was studied by time-resolved PL spectroscopy. The sample was excited by a pulsed frequency-doubled titanium sapphire laser, yielding pulses with a pulse length of 1.5 ps and a repetition rate of 82 MHz. The excitation was performed in the (Cd,Zn)Se layer with an excess energy of approximately 100 meV in order to avoid carrier capture from the ZnSe barrier. Typical excitation densities of

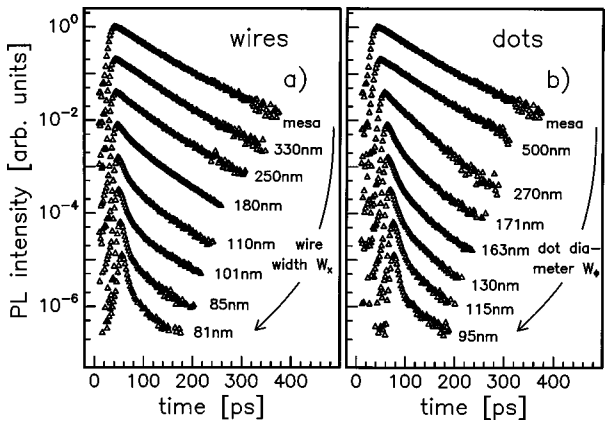

FIG. 1. Normalized PL intensity as a function of time for a set of $Cd_{0.20}Zn_{0.80}Se/ZnSe$ wires (a) and dots (b) at a temperature of 2 K.

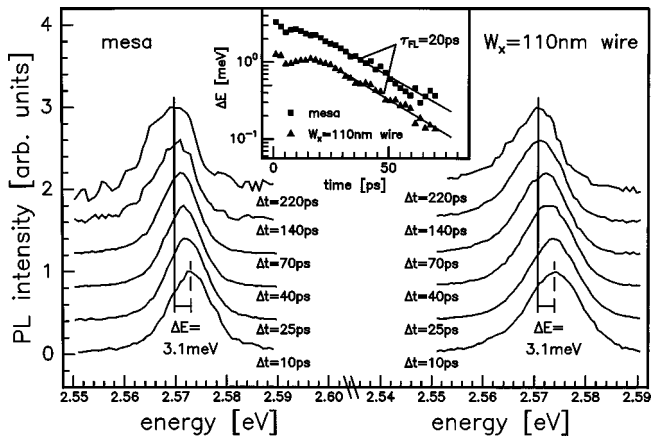

FIG. 2. Set of time-resolved PL spectra for the mesa and 110 nm wide wires at a temperature of 2 K. Inset: energy shift ΔE vs time for the mesa (squares) and the 110 nm wires (triangles, shifted vertically for clarity) in a logarithmic plot. The solid lines indicate best fits by a monoexponential law.

about 10^{10} cm^{-2} were used for all measurements if not stated otherwise. The PL signal was dispersed by a 0.32-m Jobin Yvon monochromator, and recorded using a streak camera with an S20 cathode and a subsequent charge-coupled-device array (CCD camera). The overall time resolution of the setup is about 5 ps.

III. EXPERIMENTAL RESULTS

To get insight into the recombination dynamics it is instructive to investigate the time-resolved and spectrally integrated PL signal. In Fig. 1(a) (left) the PL intensity of wires with geometrical widths W_x ranging from 330 nm to 81 nm and a two-dimensional (2D) reference (mesa) is plotted versus time for a temperature of 2 K. While the onset of the PL signal reflects carrier relaxation and exciton formation,[21] the decay is associated with the recombination of excitons. Obviously, the recombination dynamics changes if the wire width is reduced: In the case of the 2D reference and the 330 nm wires an almost monoexponential decay with a decay time of about 70 ps is obtained. In contrast, a distinct biexponential decay is observed for smaller wires where the fast component becomes shorter and more pronounced with decreasing wire width. In addition, this two-component decay characteristics strongly depends on the excitation density. While only the fast decay component is observed for exciton densities of about 10^{11} cm^{-2}, the long component becomes more pronounced if the excitation density is reduced to about 5×10^{8} cm^{-2}. Similar results were obtained for dot structures with geometrical diameters W_Φ ranging from 500 nm to 95 nm as shown in Fig. 1(b) (right). Regarding wire and dot structures with comparable lateral extensions the time constants are reduced in dots compared to wires. This indicates an enhanced nonradiative carrier loss at the etched surfaces due to the increased surface/volume ratio in dots.

Usually the lateral size dependence of the recombination dynamics in various deep etched III-V[14,16,18] and II-VI[10,17] nanostructures, respectively, is explained taking into account exciton diffusion to the sidewalls and subsequent nonradiative surface recombination. Using such a model a predominantly monoexponential decay characteristics with a size dependent time constant is obtained. Obviously, this simple diffusion model is not appropriate to explain the size-dependent biexponential decay observed in our samples. In addition, the diffusion model is also unable to explain the experimental findings in wet etched $Cd_{0.35}Zn_{0.65}Se/ZnSe$ wires,[17] where no significant reduction of the lifetime was obtained even for 20 nm wide wires.

While spectrally integrated PL transients mainly reflect the recombination dynamics of the exciton population in the structure, the analysis of time-resolved spectra gives access to relaxation, localization, or thermalization of the exciton distribution.[22,23] In Fig. 2 transient PL spectra for the mesa (left) and $W_x=110$ nm wide wires (right) are shown for a temperature of 2 K and an exciton density smaller than 10^9 cm^{-2}. For the PL maximum a time-dependent energy shift of $\Delta E=3.1$ meV to lower energies is observed for both, the mesa and the wires, reflecting the localization process of excitons due to well width and/or alloy fluctuations.[23] In the inset of Fig. 2 the transient energy shift ΔE of the PL maximum is plotted. By fitting these data using a monoexponential law (solid lines) a time constant of 20 ps was obtained in both cases reflecting the average localization time of free excitons. Hence, the data presented in Figs. 1 and 2 indicate that the recombination process of excitons in these nanostructures is influenced by both nonradiative carrier loss at the sidewalls and exciton localization.

IV. MODELING OF THE EXCITON RECOMBINATION IN ETCHED NANOSTRUCTURES

For a quantitative description of the experimental data, it seems therefore necessary to develop an extended diffusion model, which describes the interplay between exciton localization and nonradiative loss of free excitons at the sidewalls. As a first approximation, the broad exciton band usually occurring in ternary quantum wells, was separated into localized and mobile excitons.[24–26] In Fig. 3, a schematic sketch of the situation is shown. Free excitons F are formed by a generation rate $g(t)$ which includes pulsed laser excitation, carrier relaxation and exciton formation.[21] Free excitons can be captured into localized exciton states L within a time constant τ_{FL}, recombine radiatively with a recombination

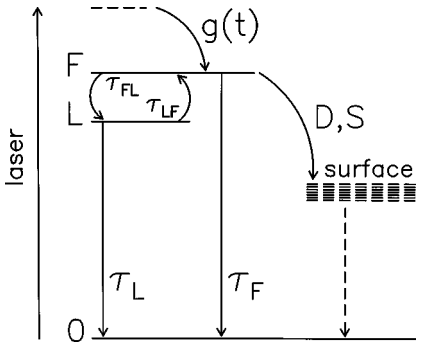

FIG. 3. Schematic sketch of the model developed in order to describe the recombination dynamics in deep etched nanostructures.

time τ_F or recombine nonradiatively at the surface. The last process is controlled by the diffusion constant D, the surface recombination velocity S, and the sample geometry, i.e., depends clearly on the wire width and the dot diameter, respectively. Localized states L can only be depopulated by a transition into free excitonic states, characterized by a transition time τ_{LF}, or by a radiative recombination process with a decay constant τ_L. Based on this model situation the following equations for the time- and space-dependent density of free and localized excitons F and L, were derived:

$$\frac{dF}{dt} = D\Delta F - \frac{F}{\tau_F} - (1 - L/N_L)\frac{F}{\tau_{FL}} + \frac{L}{\tau_{LF}} + g(t) \qquad (1)$$

$$\frac{dL}{dt} = (1 - L/N_L)\frac{F}{\tau_{FL}} - \frac{L}{\tau_L} - \frac{L}{\tau_{LF}} \qquad (2)$$

with an effective size W_{eff} for dry etched nanostructures including a deadlayer W_D:[13]

$$W_{\text{eff}} = W_i - 2W_D \qquad (3)$$

and the boundary condition:

$$D\frac{dF}{dr}\bigg|_{r=\pm(W_{\text{eff}}/2)} = -SF|_{r=\pm(W_{\text{eff}}/2)} \qquad (4)$$

$$\text{wires:} \quad r = x$$

$$\text{dots:} \quad r = \sqrt{x^2 + y^2}\,.$$

W_i $(i = x, i = \Phi)$ is the geometrical lateral extension of the structure, i.e., the wire width W_x and the dot diameter W_Φ, respectively. Δ describes the Laplace operator for one (wires) or two (dots) dimensions, respectively. N_L corresponds to the density of localized states and the factor $1 - L/N_L$, which takes into account the finite number of localized states, describes saturation effects for enhanced exciton densities.[27] These equations were solved numerically for wire and dot structures and the spectrally integrated PL intensity was calculated by:

$$I(t) = \frac{d(F+L)}{dt}\bigg|_{\text{radiative}} = \frac{F}{\tau_F} + \frac{L}{\tau_L}. \qquad (5)$$

To demonstrate the influence of the density of localized states N_L and the transition rate τ_{LF}^{-1} on the recombination

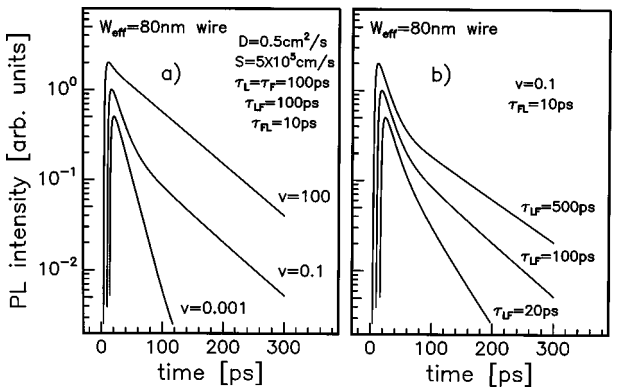

FIG. 4. Model calculations of the transient PL signal for a wire with an effective width $W_{\text{eff}} = 80$ nm according to Eqs. (1)–(5). (a) Variation of the ratio v between density of localized states N_L and laser generated exciton density G. (b) Variation of the depopulation time τ_{LF}. The time constants used for the simulations are given in the figure.

dynamics, the results of the corresponding simulations are presented in Fig. 4. In Fig. 4(a) (left) the calculated PL intensity for a wire with an effective width $W_{\text{eff}} = W_x - 2W_D = 80$ nm is displayed for different values of $v = N_L/G$ by using a typical set of parameters as given in the figure. Here G, the number of laser generated excitons per area and per pulse, is kept constant.

If the density of localized states is much smaller than the number of generated excitons per unit area (corresponding to $v = 0.001$), a monoexponential decay is obtained with a characteristic time constant of 20 ps, i.e., significantly reduced as compared to the 2D reference. In this case, a distinct reduction of the time constant with decreasing wire width is found. This indicates that the excitons behave like free excitons mainly undergoing nonradiative recombination at the sidewalls. Thus, the size-dependent exciton lifetimes in wires and dots are mainly controlled by the diffusion constant D and the surface recombination velocity S. Experimentally, this situation is realized, e.g., for GaAs/(Al,Ga)As wires or ZnSe/Zn(S,Se) wires as reported in the literature.[16,17]

In contrast, if the density of localized states N_L exceeds the number of excitons per unit area significantly (corresponding to $v = 100$) an almost monoexponential decay within a time constant given by the radiative lifetime of localized excitons is obtained. In this case, the decay time is found to be independent of the wire width. This indicates that free excitons mainly become localized before reaching the surfaces, resulting in a suppression of non-radiative carrier loss at the wire sidewalls. Experimentally, such a behavior was observed in wet etched $Cd_{0.35}Zn_{0.65}Se/ZnSe$ wire structure, as reported recently.[17,19] At this point, it is instructive to discuss the size dependence of the normalized PL intensity for this situation, which can be evaluated easily from our calculations. Although no reduction of the exciton recombination time is obtained for decreasing wire width, carrier loss at the wire sidewalls can occur during the relaxation process of excitons into localized states, reducing the PL intensity in narrow wires.[17,28]

In contrast, a biexponential decay is obtained, if the density of localized states N_L is almost comparable to the density of photogenerated excitons ($v = 0.1$). Immediately after

excitation, the exciton density exceeds the density of localized states and therefore the fast component of the decay characteristics reflects the nonradiative carrier loss of free excitons at the sidewalls. After approximately 100 ps, the recombination of localized excitons dominates the decay characteristics, resulting in a time constant, which is almost independent on the wire width. This situation is realized for the exciton recombination in wires and dots presented in Fig. 1, indicating the necessity of including exciton localization in the model calculations in order to discuss our experimental data quantitatively. Moreover, the theoretically obtained variation of the decay characteristics with $v = N_L/G$ is able to reproduce the experimental data for different excitation densities, as discussed above.

It is well known that an efficient depopulation of localized states can be obtained, e.g., by increasing the temperature.[27] This can be simulated in our calculations by decreasing the depopulation time τ_{LF} between localized and free exciton states. In Fig. 4(b) (right) the PL signal of an 80 nm wide wire structure is plotted versus time for various values of τ_{LF}. For $\tau_{LF} = 500$ ps a distinct biexponential decay with time constants of 20 ps and 90 ps, respectively, is obtained. Decreasing the transfer time τ_{LF} e.g., to 20 ps, the long component of the decay is reduced significantly to 40 ps. This indicates that by increasing the depopulation rate τ_{FL}^{-1} a reduction of the effective lifetime of localized excitons and in increase of the nonradiative carrier loss is obtained due to the coupling of localized excitons to nonradiative surface states via free exciton states. This also becomes apparent in a reduction of the normalized PL intensity, which decreases, e.g., by about 20% by reducing τ_{LF} from 500 ps to 20 ps.

V. DISCUSSION

In order to permit a quantitative description of the experimental data as much as possible of the model parameters should be determined experimentally. By evaluating the time-resolved PL signal of the 2D reference at $T = 2$ K the recombination time as well as the localization time τ_{FL} can be derived. Low excitation densities are used in order to avoid any saturation effects of the localized states. Thus, the decay time constant reflects the recombination lifetime τ_L of localized excitons, while the transient energy shift of the PL spectrum after pulsed excitation is mainly controlled by the localization time τ_{FL} as shown in Fig. 2. From the experiments, $\tau_L = 70$ ps and $\tau_{FL} = 20$ ps, respectively, can be deduced. As a first approximation the same recombination time is used for the lifetime of free excitons at low temperatures. In addition a dead layer with a width $W_D = 20$ nm and a surface recombination velocity $S = 2.5 \times 10^5$ cm/s were used as reported in Refs. 9 and 20, respectively, for dry-etched (Cd,Zn)Se/ZnSe nanostructures.

With this approach the number of fitting parameters is strongly reduced. As discussed above the fast component of the decay, representing the size-dependent nonradiative loss of free excitons via surface states, is mainly influenced by D, S, and W_{eff}, whereas the exciton localization process is controlled by N_L and τ_{LF}. In order to achieve the absolute density of localized states N_L, the number of laser-generated excitons per area and per pulse has to be determined. This was done as described in Ref. 7 taking into account the excitation density of the laser pulse. An absorption coefficient of 2.5×10^4 cm^{-1} was used as reported for a comparable structure in Ref. 29.

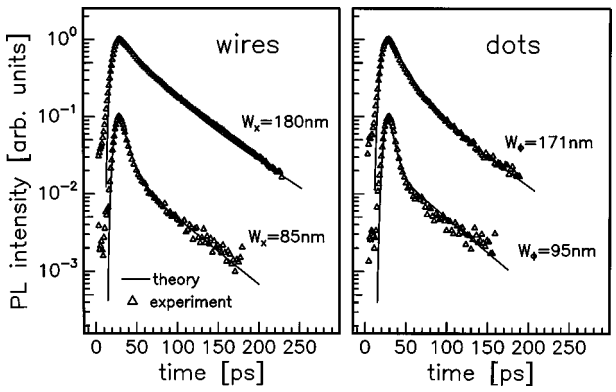

FIG. 5. PL intensity as a function of time (triangles) and best fits (solid lines) for a set of wire and dot structures at $T = 2$ K.

In Fig. 5 best fits (solid lines) for a set of wire (a) and dot (b) structures are compared to the experimental data (triangles) for $T = 2$ K. The experimental data of both, the wires and the dots are described by one set of parameters. Excellent agreement between the experimental data and the model calculations is found. Especially, the experimentally observed transition from a monoexponential decay for the 2D reference to the biexponential decay characteristics observed for narrow wires and dots is reproduced quite well.

From these fits a diffusion constant of $D = 0.6$ cm^2/s is obtained. Comparable values for D were reported for other deep etched nanostructures based on ZnSe.[17] Moreover, an estimate of the density of localized states is possible. We obtain $N_L = 7 \times 10^8$ cm^{-2}, a value that seems to be quite low. Spatial fluctuations of the alloy and/or the well width are expected to build up a potential landscape with energy variations on different length scales, often separated into long-range and short-range contributions.[24,30] Thus, we attribute long-range fluctuations responsible for the localization of excitons in our samples. This is in agreement with the finite localization time τ_{FL}, which clearly indicates, that the excitons move several tens of nm (i.e., much more than the exciton diameter) before becoming localized. Of course the interface structure strongly depends on the growth conditions. It has been shown, e.g., by Rabe *et al.*,[31] that much higher values of N_L can be obtained changing the growth mode, indicating the transition from a quasi-two-dimensional growth mechanism to the Stranski-Krastanow growth of self-organized quantum dots.[31]

By increasing the temperature, a thermally induced depopulation of localized states is expected. This should be controlled by a characteristic activation energy corresponding to the average localization energy of excitons. In order to investigate this mechanism an analysis of the exciton recombination dynamics is performed for temperatures between 2 K and 80 K.

In the inset of Fig. 6 the decay curves of wire structures with a geometrical width $W_x = 110$ nm are plotted for temperatures of $T = 20$ K and 60 K, respectively (triangles). The main result is the vanishing of the long component of the decay characteristics by increasing the temperature. For the modeling, the same values of N_L and τ_{FL} were used as de-

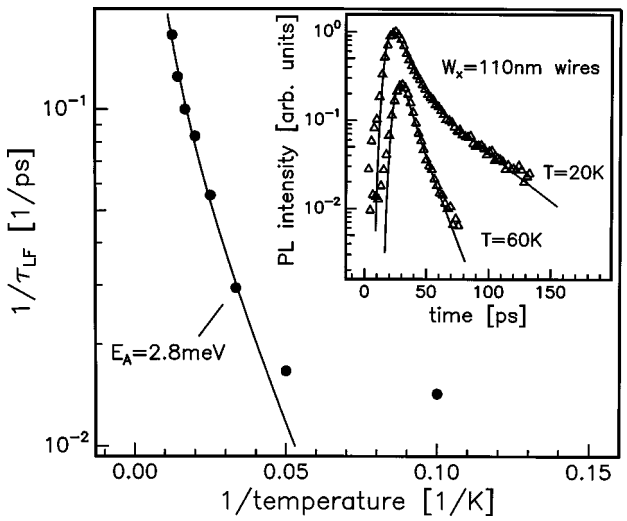

FIG. 6. Arrhenius-plot of the depopulation rate τ_{LF}^{-1} from localized into free-exciton states. The solid line represents the best fit according to Eq. (6). Inset: Transient PL intensity (triangles) and best fits (solid lines) for wires with a geometrical width $W_x = 110$ nm at $T = 20$ K and 60 K, respectively.

rived at $T = 2$ K. In addition, the temperature dependence of S was derived by the Stevenson-Keyes formula[14,32] and the exciton lifetime was deduced from the 2D reference. Best fits are shown as solid lines, yielding accurate values for the temperature dependence of the diffusion constant D and the depopulation time τ_{LF}. For the diffusion constant, an increase from $D = 0.6$ cm^2/s at $T = 2$ K to $D = 1.6$ cm^2/s at $T = 60$ K is found corresponding to an enhancement of the diffusion length from 65 nm to 150 nm. A similar behavior was also reported for the lateral diffusion of excitons in GaAs/(Al,Ga)As quantum wells[21] and explained by both, the temperature dependence of the exciton scattering mechanisms and the exciton lifetime.

Of special interest is the temperature dependence of the depopulation rate τ_{FL}^{-1}, which should give access to the average localization energy. In Fig. 6, τ_{FL}^{-1} is displayed as a function of the inverse lattice temperature in an Arrhenius plot. With increasing temperature, a distinct enhancement of τ_{FL}^{-1}, e.g., from 0.02 ps^{-1} for $T = 20$ K to 0.1 ps^{-1} for $T = 60$ K is found. Assuming thermal equilibrium between free and localized states the temperature dependence of the ratio between the localization rate τ_{FL}^{-1} and the depopulation rate τ_{LF}^{-1} is expected to be:[27]

$$\tau_{LF}/\tau_{FL} \propto T e^{-E_A/kT} \tag{6}$$

where E_A is an activation energy for the thermally induced transition from localized to free-exciton states representing an average localization energy. Fitting the experimental data in the temperature range from 30 K to 80 K by this expression we determine an activation energy of $E_A = 2.8$ meV. This value can be compared to the transient energy shift of the PL maximum at very low exciton densities (see Fig. 2), which was found to be 3.1 meV. The good agreement of both values indicates that the assumption of a thermal equilibrium holds at least for temperatures larger than 30 K. The reason for the deviation between the experimental data and Eq. (6) at low temperatures is not yet clear. One might expect, that thermal equilibrium is not established at low temperatures due to the finite relaxation time of excitons.

VI. CONCLUSIONS

The recombination dynamics of excitons in dry etched (Cd,Zn)Se/ZnSe nanostructures was investigated by time-resolved PL spectroscopy. For wire widths and dot sizes smaller than about 300 nm and 200 nm, respectively, the recombination characteristics of the exciton signal changes from a monoexponential to a biexponential decay. In order to explain the experimental findings quantitatively an extended diffusion model was proposed, including the interplay between exciton localization and nonradiative carrier loss of free excitons at the sidewalls.

A good agreement between the experimental data of the recombination dynamics of excitons in dot and wire structures with different lateral extension and the model calculations is obtained by using one set of parameters. From the data, a density of localized states $N_L = 7 \times 10^8$ cm^{-2} and an activation energy $E_A = 2.8$ meV, describing the average localization energy of excitons are obtained. Besides an excellent description of the experimental data presented here, the model is able to reproduce the various experimental findings of the size-dependent exciton recombination dynamics reported in the literature, giving a consistent picture for the recombination process of excitons in deep etched nanostructures.

ACKNOWLEDGMENTS

We would like to thank M. Emmerling for expect technical assistance. We gratefully acknowledge the financial support of this work by the Deutsche Forschungsgemeinschaft (Grant No. SFB410). The work in Linz was supported by FWF, GME, and BMWV, Vienna.

[1] J. Hegarty, K. Tai, and W. T. Tsang, Phys. Rev. B **38**, 7843 (1988).
[2] E. Runge, A. Schülzgen, F. Henneberger, and R. Zimmermann, Phys. Status Solidi B **188**, 547 (1995).
[3] F. J. Stützler, S. Fujieda, M. Mizuta, and K. Ishida, Appl. Phys. Lett. **53**, 1923 (1988).
[4] T. Takagahara and E. Hanamura, Phys. Rev. Lett. **56**, 2533 (1986).
[5] J. Bergman, P. Holtz, B. Monemar, M. Sudaram, J. Merz, and C. Cossard, Phys. Rev. B **43**, 4765 (1991).
[6] G. Bacher, H. Schweizer, J. Kovac, H. Nickel, W. Schlapp, and R. Lösch, Appl. Phys. Lett. **61**, 702 (1992).
[7] R. Spiegel, G. Bacher, A. Forchel, B. Jobst, D. Hommel, and G. Landwehr, Phys. Rev. B **55**, 9866 (1996).
[8] M. G. Bawendi, W. L. Wilson, L. Rothberg, P. J. Caroll, T. M. Jedju, M. L. Steigerwald, and L. E. Brus, Phys. Rev. Lett. **65**, 1623 (1990).
[9] J. Ding, A. V. Nurmikko, D. C. Grillo, Li He, J. Han, and R. L.

Gunshor, Appl. Phys. Lett. **63**, 2254 (1993).
[10] H. Mariette, C. Gourgon, J. Cibert, Le Si Dang, C. Vieu, G. Brunthaler, H. Straub, W. Faschinger, N. Pelekanos, and W. W. Rühle, in *Semiconductor Heteroexpitaxy: Growth, Characterization and Device Applications*, edited by B. Gil and R. L. Aulombard (World Scientific, Singapore, 1995), p. 383.
[11] M. Illing, G. Bacher, A. Forchel, T. Litz, A. Waag, and G. Landwehr, Appl. Phys. Lett. **66**, 1815 (1995).
[12] T. Kümmell, G. Bacher, A. Forchel, J. Nürnberger, W. Faschinger, G. Landwehr, B. Jobst, and D. Hommel, Appl. Phys. Lett. **71**, 344 (1997).
[13] B. E. Maile, A. Forchel, R. Germann, and D. Grützmacher, Appl. Phys. Lett. **54**, 1552 (1989).
[14] G. Mayer, B. E. Maile, R. German, A. Forchel, P. Grambow, and H. P. Meier, Appl. Phys. Lett. **56**, 2016 (1990).
[15] J. Crank, *The Mathematics of Diffusion* (Clarendon, Oxford, 1975), p. 79.
[16] A. Izrael, B. Sermage, J. Y. Marzin, A. Ougazaden, R. Azoulay, J. Etrillad, V. Thierry-Mieg, and L. Henry, Appl. Phys. Lett. **56**, 830 (1990).
[17] R. Spiegel, G. Bacher, K. Herz, M. Illing, T. Kümmell, A. Forchel, B. Jobst, D. Hommel, G. Landwehr, J. Söllner, and M. Heuken, Phys. Rev. B **53**, R4233 (1996).
[18] E. M. Clausen, Jr., H. G. Craighead, J. M. Worlock, J. P. Harbison, L. M. Schiavone, L. Florez, and B. Van der Gaag, Appl. Phys. Lett. **55**, 1427 (1989).
[19] R. Spiegel, G. Bacher, K. Herz, M. Illing, T. Kümmell, A. Forchel, B. Jobst, D. Hommel, and G. Landwehr, Nuovo Cimento D **17**, 1729 (1995).
[20] H. Straub, G. Brunthaler, G. Bauer, and C. Vieu, J. Cryst. Growth **159**, 51 (1996).
[21] H. Hillmer, A. Forchel, S. Hansmann, M. Morohashi, E. Lopez, H. P. Meier, and K. Ploog, Phys. Rev. B **39**, 10 901 (1989).
[22] F. Yang, M. Wilkinson, E. J. Austin, and K. P. O'Donnel, Phys. Rev. Lett. **70**, 323 (1993).
[23] G. Bacher, R. Spiegel, T. Kümmell, O. Breitwieser, A. Forchel, B. Jobst, D. Hommel, and G. Landwehr, Phys. Rev. B **56**, 6868 (1997).
[24] U. Jahn, M. Ramsteiner, R. Hey, H. T. Grahn, E. Runge, and R. Zimmermann, Phys. Rev. B **56**, R4387 (1997).
[25] R. Zimmermann and E. Runge, Phys. Status Solidi A **164**, 511 (1997).
[26] J. Hegarty, L. Goldner, and M. D. Struge, Phys. Rev. B **30**, 7346 (1984).
[27] C. I. Harris, B. Monemar, H. Kalt, P. O. Holtz, M. Sundaram, J. L. Merz, and A. C. Gossard, Phys. Rev. B **50**, 18 367 (1994).
[28] M. Illing, G. Bacher, T. Kümmell, A. Forchel, D. Hommel, B. Jobst, and G. Landwehr, J. Vac. Sci. Technol. B **13**, 2792 (1995).
[29] J. Ding, N. Pelekanos, A. V. Nurmikko, H. Luo, N. Samarth, and J. K. Furdyna, Appl. Phys. Lett. **57**, 2885 (1990).
[30] D. Bennhardt, P. Thomas, A. Weller, M. Lindberg, and S. W. Koch, Phys. Rev. B **43**, 8934 (1991).
[31] M. Rabe, M. Lowisch, F. Kreller, and F. Henneberger, Phys. Status Solidi B **202**, 817 (1997).
[32] D. T. Stevenson and R. J. Keyes, Physica **20**, 104 (1954).